

Phase transitions and critical phenomena of tiny grains carbon films synthesized in microwave-based vapor deposition system

Mubarak Ali ^{a,*} and I-Nan Lin ^b

^a Department of Physics, COMSATS Institute of Information Technology, Islamabad 45550, Pakistan. *E-Mail: mubarak74@comsats.edu.pk, mubarak74@mail.com

^b Department of Physics, Tamkang University, Tamsui Dist., New Taipei City 25137, Taiwan

Abstract –Different peak trends in tiny grains carbon film have been observed under the investigations of Raman spectroscopy and energy loss spectroscopy. Carbon films known in nanocrystalline and ultra-nanocrystalline diamond films are synthesized by employing microwave-based vapor deposition system. Carbon atom deals several state behaviors depending on the incurred positions of electrons. This results into evolve tiny grains having different phases in the film. Those tiny grains of carbon film evolved in graphitic state atoms, they converted to structure of smooth elements where elongation of atoms of one-dimensional arrays is as per exerting surface format force along opposite poles from their centers. Such tiny grains are the cause of ν_1 peak in the Raman spectrum of their film because of enhanced propagation of input laser signals through channelized inter-state electron gap of uniformly elongated atoms. Those tiny grains of carbon film evolved in fullerene state of atoms, they are the cause of ν_2 peak. The tiny grains of ν_1 peak possess its low intensity as compared to the ones comprised atoms having state behaviors known in exceptional hardness. Tiny grains of ν_1 peak are also the cause of enhanced field emission characteristics of a carbon film. Interacting laser beam to certain region of film recording peaks at different wave numbers indicating different state behavior of atoms for each phase of tiny grains, namely, graphitic state, lonsdaleite state, diamond state, fullerene state and graphene state where revealing not a different behavior for energy loss spectroscopy of that film.

Keywords: Tiny grains carbon films; Photon and heat energy; Phase transition; Raman spectra; Field emission; Energy loss spectroscopy

1.0 Introduction

Developing materials in selective size and decorum along with investigating their characteristics at precise detail requires a new sort of approaches and observations. Phase transition of carbon atoms while developing a film is a usual phenomenon but it is crucial to pinpoint where may be the origin of different characteristic not yet disclosed, and if disclosed, it can be under the different flourishing explanation of underlying science. Switching dynamics of morphology-structure in carbon films under varying process conditions has been discussed elsewhere [1].

The syntheses of nanocrystalline diamond (NCD) and ultrananocrystalline diamond (UNCD) films only span over few decades where interplay of varying process conditions in the presence of different concentrations of feed gases (methane, hydrogen and argon, etc.) in microwave plasma chemical vapor deposition (MPCVD) or microwave plasma enhanced (MPE)-CVD are the source of their development. The characteristics of NCD/UNCD films are mainly recognized in terms of Raman spectroscopy, energy loss spectroscopy and microscopic observations, whereas, their performance is mainly recognized in terms of field emission characteristics. The NCD/UNCD films mainly deal tiny grains, size ranging tens of nanometer to few nanometers.

It is necessary to understand dynamics of tiny particles' formation prior to go for assembling into large size particles [2]. Agglomerations of colloidal matter envisage atoms and molecules to deal them as materials for tomorrow [3]. Developing different tiny particles of gold has been discussed elsewhere [4]. The development mechanism of tiny shaped particles under varying precursor concentration has been discussed [5]. Under identical process parameters, the nature of precursor directs tiny shaped particles following by large shaped particles where role of atomic nature is crucial [6]. Different tiny shaped particles were developed under the packets of nano shape energy while varying the ratio of bipolar pulse OFF to ON time [7]. Formation process of large-sized particles reveals very fast development rate [8]. In certain nature atoms, their binding to evolve different-dimension and different-formats structures take place under the execution of confined inter-state electron-dynamics where conservative forces involved in the shaping of different characteristic energies as discussed elsewhere [9]. Tiny shaped particle deals localized gravity of mono layer in developing large shaped particle [10]. Atoms of suitable elements which execute electronic transitions don't ionize, deform or

elongate while inert gas atoms split under the surplus propagation of photonic current [11]. The phenomena of heat and photon energy have been discussed while considering the neutral state silicon atom [12]. Influence of deposition chamber pressure has been discussed in depositing carbon films of content-specific growth in hot-filaments deposition unit [13]. Working of tiny-sized particles for diligent application, they may have pronounced effect to work either effective nanomedicine or defective because of certain nature of comprised atoms [14].

Electron field emission (EFE) device fabricated by heating tiny diamond grains in hydrogen plasma reveals high characteristic, which is due to the high defect density and low electron affinity [15]. Increasing nitrogen content slightly increases sp^2 -bonding in grain-boundary and local bonding structure remains the same [16]. Diverse geometries coupled with varieties of attachment sites enabling diamondoids as useful building blocks for molecular-design applications [17]. Size of grains in UNCD film in the range of 2-3 nm remains thermodynamically stable as tested under broad range of pressure –temperature of hydrogenated surfaces [18]. Grains in nanometer size indicate specific changes because of the decreased mobile dislocations and below their critical size, a softening behavior is often observed, and change is triggered by atomic shuffling where simulation approaches are incapable to evaluate underlying mechanism [19]. Sumant *et al.* [20] investigated the surface chemistry and nanotribology inside the UNCD films and are indistinguishable chemically, adhesively and tribologically from single-crystal diamond.

Several studies of UNCD films are available in the literature targeting field emission characteristics under different process parameters along with varying concentration of gases (and dopants as well). On increasing the local density of states, UNCD films provide conducting path at diamond-vacuum interface [21]. UNCD films synthesized at low temperatures and in nitrogen environment demonstrated high conductivity in their various applications [22]. Under nitrogen atmosphere, the grain size of UNCD film becomes smaller than 10 nm and metallic conductivity is achieved [23]. UNCD film has low friction/wear and rapid passivation of dangling bonds is a matter of concern in humid environment [24]. UNCD films are different as compared to NCD films in several ways such as their grain sizes are 2 nm to 5 nm, they are bound by sp^2 -carbon and usually grow in argon-rich/hydrogen-poor CVD environment and may contain 95–98% sp^3 -bonded carbon [25]. In UNCD films, homojunction facilitates the tunneling of electrons in conduction band and their

direct transport at conducting/insulating interface [26]. To synthesize diamond films at temperatures below 600°C, UNCD films are superior in choice because their properties don't degrade as in polycrystalline diamond films [27]. On increasing substrate temperature along with hydrogen concentration in Ar/CH₄ plasma, *sp*³-diamond phase becomes less passivated [28]. Low friction coefficient of UNCD films is linked with large amounts of hydroxylic/carboxylic functional groups which are recognized as grain boundary [29]. Bias enhanced nucleation/growth processes facilitate the transport of graphitic phase in both the interior and interface regions of UNCD films [30]. Hydrogen concentration increases the size of diamond grains [31]. Boron-doped UNCD films are capable of being utilized in the field of atomic force microscopy/robust electrodes/bio-compatible sensors [32]. On lowering the a-C layer at interface UNCD/Au-Si composite structure delivers better conductivity and improves EFE [33]. Precise growth of sub-2 nm/above 5 nm sized diamond grains is achieved due to energetic species under low growth temperature and pre-nucleated interface, thus, tiny grains on silicon nanoneedles deliver enhanced EFE [34]. Gold-UNCD films show superior EFE properties than copper-UNCD films and authentic factor underneath the mechanism is the presence of nanographitic phases [35]. Copper ion implantation and annealing process increase the EFE due to the improved conducting nature of UNCD films [36]. Presence of graphitic phases at the interfaces of ZnO nanorods/UNCD needles decreases the resistivity of layer and core-shell heterostructures, thus, delivered superior EFE [37]. Nitrogen-incorporated UNCD grains serve as 'high-density diamond nuclei' in the hybrid carbon film [38]. In all those studies and many others, factors related to performance of UNCD/NCD films are linked with the tiny grains of UNCD/NCD films. Improvement in the conductivity but not EFE of P-ions incorporated-UNCD films was due to the transportation of electrons crossing interface [39]. Transportation of electrons is the prime reason for enhanced conductivity and field emission of doped films [40].

In the present work, different 'tiny grains carbon films' are synthesized in microwave-based vapor deposition system known in MPCVD or MPE-CVD system. Formation process of 'tiny grains carbon films' is discussed under the variation of chamber pressure and different concentration of hydrogen gas. Raman spectroscopy and energy loss spectroscopy analyses of films reveal different intensity of peaks along with different trend. Additionally, a film synthesized for same parameters show a bit different information of obtained data when analysis is under its different

locations. These indicate that 'tiny grains carbon films' deal miscellaneous behaviors of their structure. Raman spectroscopy and energy loss spectroscopy analyses of 'tiny grains carbon films' tally each other along with their field emission characteristics. The performance of carbon films in terms of tiny grains comprised arrays of graphitic state atoms is pinpointed.

2.0 Experimental details

To synthesize 'tiny grains carbon films', microwave-based vapor deposition system (IPLAS-Cyrannus, 2.45 GHz) was employed. A schematic of deposition system is given elsewhere [41]. Silicon wafers N-type nature ($\rho \sim 1-5 \text{ Ohm-cm}$) were used as a substrate. Initial duration of the nucleation process was set 30 minutes, whereas, deposition time was set 60 minutes. Prior to load the samples in the chamber, substrates were cleaned by ultrasonic agitation for the duration of 30 minutes in methanol solution containing nanodiamond powders size $\sim 30 \text{ nm}$ and titanium powders of 325 meshes to create nucleation sites. The total mass flow rate was 200 sccm and was kept constant. The substrate temperature was measured by K-type thermocouple where 6 % H_2 in argon –rich methane mixture was used to synthesize carbon films and the recorded value was $700^\circ\text{C} \pm 10^\circ\text{C}$, whereas, it was significantly lowered in films synthesized without H_2 where the value was $500^\circ\text{C} \pm 10^\circ\text{C}$. On increasing chamber pressure from 100 torr to 200 torr at constant microwave power 1400 (watts), no significant difference in temperature was noted. Due to the lower thermal conductivity of Ar than H_2 , heating of substrate by plasma is greatly reduced in argon-rich CH_4 mixture [22]. Surface morphology of films were analyzed by scanning microscope (ZEISS Model: SIGMA). Peaks related to different nature tiny grains were identified by Raman spectroscopy analysis (Renishaw; 325 nm and HR800 UV; 632.8 nm). Photon field emission (PFE) of films, which is known in electron field emission, were deduced by using a tunable parallel plate set-up known in $I-V$ curve and measurements were made by employing an electrometer (Keithley 237) under vacuum level of 10^{-6} torr. Dark field, bright field, high-resolution images and selected area photon reflection (SAPR) patterns (known in SAED) of films were taken by high-resolution microscope (HR-TEM, JEOL JEM2100F) operated at 200 kV. Energy of different bands of films was deduced by core loss photon energy loss spectroscopy (core loss PELS) and low loss photon energy loss spectroscopy (low loss PELS), which are known in core loss EELS and low loss EELS.

3.0 Results and discussion

Raman spectra of different 'tiny grains carbon films' synthesized at 100 torr, 150 torr and 200 torr are shown in Figure 1, which show different intensity levels of 'v₁ peak'. The 'v₁ peak' in films synthesized at 100 torr and 200 torr is more pronounced as compared to the one in film synthesized at 150 torr. The 'v₁ peak' is intensive in film synthesized without H₂ gas (Figure S1) as compared to the films synthesized at 6% H₂ (in Figure 1); morphology of film having Raman spectrum in Figure S1 is shown in Figure S2. In different Raman spectra, the 'v₁ peak' at wave number ~1150 cm⁻¹ is at low level of intensity as compared to D*, D and G peaks. Field emission current density (in known units) as a function of applied field (in known units) at different chamber pressures is shown in Figure 2. Film synthesized at 100 torr shows superior field emission properties where 'turn on field' is 11.52 V/μM (the lowest value) and the large current density (> 2.0 mA/cm²). The 'turn on field' was the highest (25 V/μM) in the film synthesized at 150 torr, whereas, it is recorded 16.4 V/μM at 200 torr. Surface morphology of 'tiny grains carbon films' synthesized at different chamber pressures are shown in Figures S3 (a) to S3 (c); at 150 torr, more tiny grains are in needle-like shapes. In films synthesized at 100 torr and 200 torr, tiny grains are composed more like in the shape of tiny clusters. Morphology of tiny grains synthesized without H₂ gas as shown in Figure S2 is identical to the ones in film synthesized at 6 % H₂ as shown in Figure S3 (b).

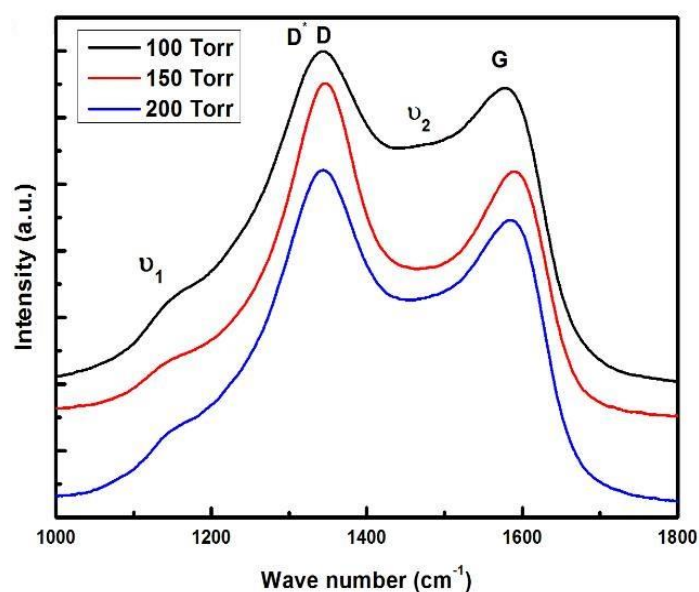


Figure 1: Raman spectra of 'tiny grains carbon films' synthesized at chamber pressure 100 torr, 150 torr and 200 torr; total mass flow rate: 200 sccm (6% H₂, 1 % CH₄ and 93 % argon, Ar: CH₄: H₂ = 186:2:12), microwave power: 1400 (in watts) and deposition time: 60 minutes

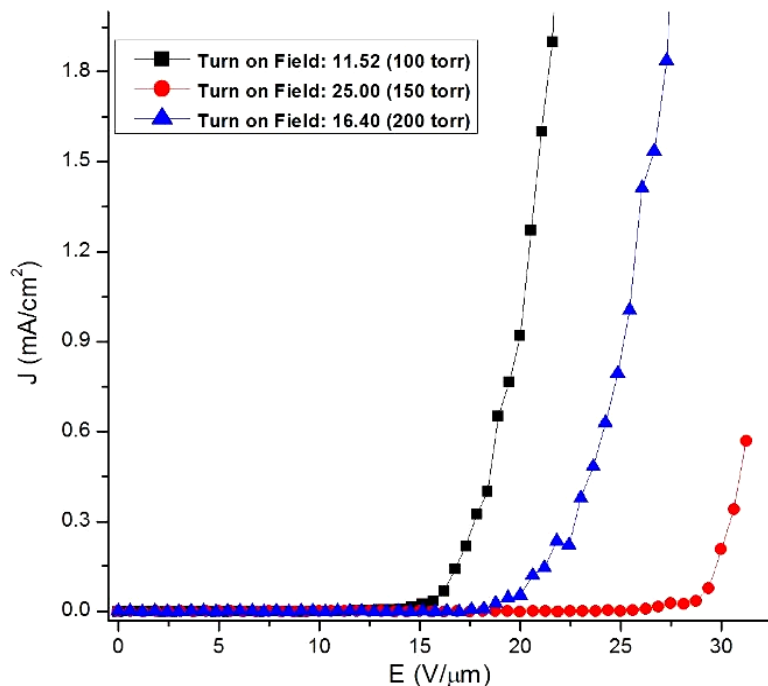


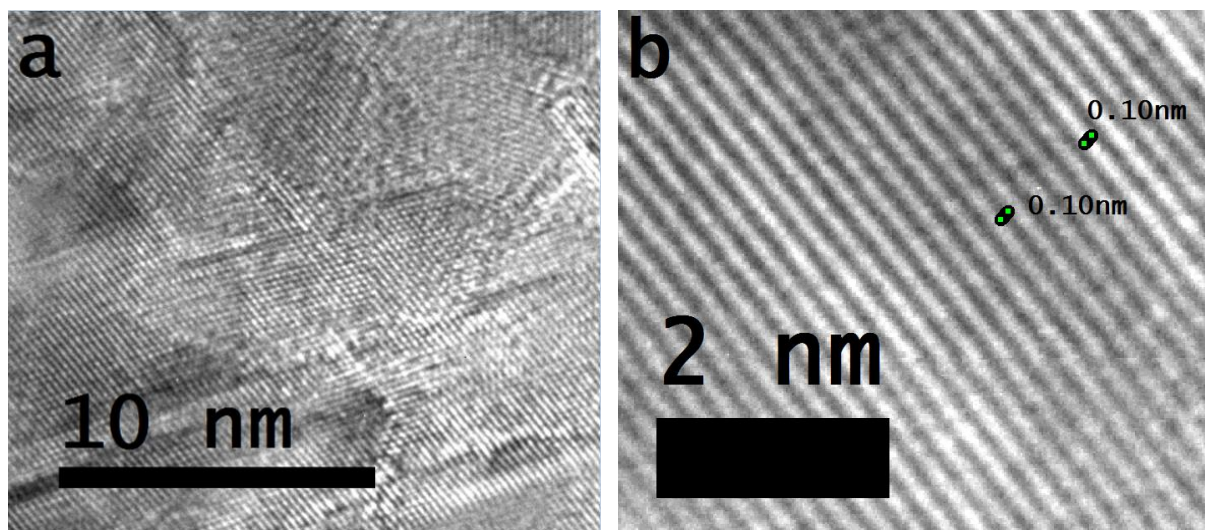
Figure 2: Field emission current density of ‘tiny grains carbon films’ synthesized at chamber pressure 100 torr, 150 torr and 200 torr as a function of applied field; total mass flow rate: 200 sccm (6% H₂, 1 % CH₄ and 93 % argon, Ar: CH₄: H₂ = 186:2:12), microwave power: 1400 (in watts) and deposition time: 60 minutes

Field emission current density of different ‘tiny grains carbon films’ synthesized in Ar-rich CH₄ mixture without H₂ and with H₂ (3% and 6%) as a function of applied field are shown in Figures S4 (a-c). In Figures S4 (a) to S4 (c), the general trend of the ‘turn on field’ is more morphology-dependent; the value of ‘turn on field’ at 100 torr is lower than that at 150 torr (same trend in Figure 2). Under lower chamber pressure (at 100 torr), all films in Figure S4 (a-c) show lower ‘turn on field’ where more number of tiny grains elongated atoms to structure of smooth elements as low ‘turn on field’ value was measured due to the enhanced and accelerated propagation of photonic current, whereas, the large value of ‘turn on field’ in the film synthesized at 200 torr (Figure S4a) is appeared to be related to less number of tiny grains converted (modified) their structure to structure of smooth elements.

Dark field transmission microscope images of ‘tiny grains carbon films’ synthesized at 100 torr and 200 torr are shown in Figures S5 (a) and S6 (a) where small-sized dark spots are related to isolated tiny grains and bigger dark spots are related to coalesced tiny grains where they packed under the exertion of changing force behaviors and contrast is more visible in bright field transmission microscope images shown in Figures S5 (b) and S6 (b); in some regions of the film, tiny grains

amalgamated and in some regions of the film, tiny grains dispersed. SAPR patterns taken at the same regions of films (shown in Figures S5b and S6b) are shown in Figures S5 (c) and S6 (c) where intensity spots don't show precise rings related to one phase indicating the presence of different-phase tiny grains. As indicated in the marked scale which is nearly a half of the nanometer where photons reflected at the surface of mixed behavior structure don't reveal any specific order in spotted dots of intensity, which is the same case in other pattern as well.

High-resolution transmission microscope image taken from 'tiny grains carbon film' synthesized at 100 torr is shown in Figure 3 (c) and from the figure two regions of magnified images are shown in Figures 3 (a) and 3 (b). In Figure 3 (c), several tiny grains show elongation of one-dimensional arrays of atoms to structure of smooth elements, which are originally related to graphite structure. The elongation of graphitic state atoms is as per stretching of clamping energy knots to electrons as their increased orientational force along the east-west poles as discussed elsewhere [42]. In the image shown in Figure 3 (a), atoms of the most of underlying tiny grains (also those at the surface) are appeared to be elongated converted each one-dimensional array in structure of smooth element. In Figure 3 (b), a single tiny grain is shown in which all atoms of one-dimensional arrays elongated uniformly resulting into convert structure of one-dimensional arrays to structure of smooth element. In Figure 3 (c), different textures of tiny grains indicate their different phases evolved in the film where more tiny grains developed in structure of smooth elements on elongating atoms of one-dimensional arrays. In the deposition chamber, travelling photons of adequate wavelnegth further shaped such tiny grains having structure of smooth elements to align inter-state electron gap for accelerated propagation of field.



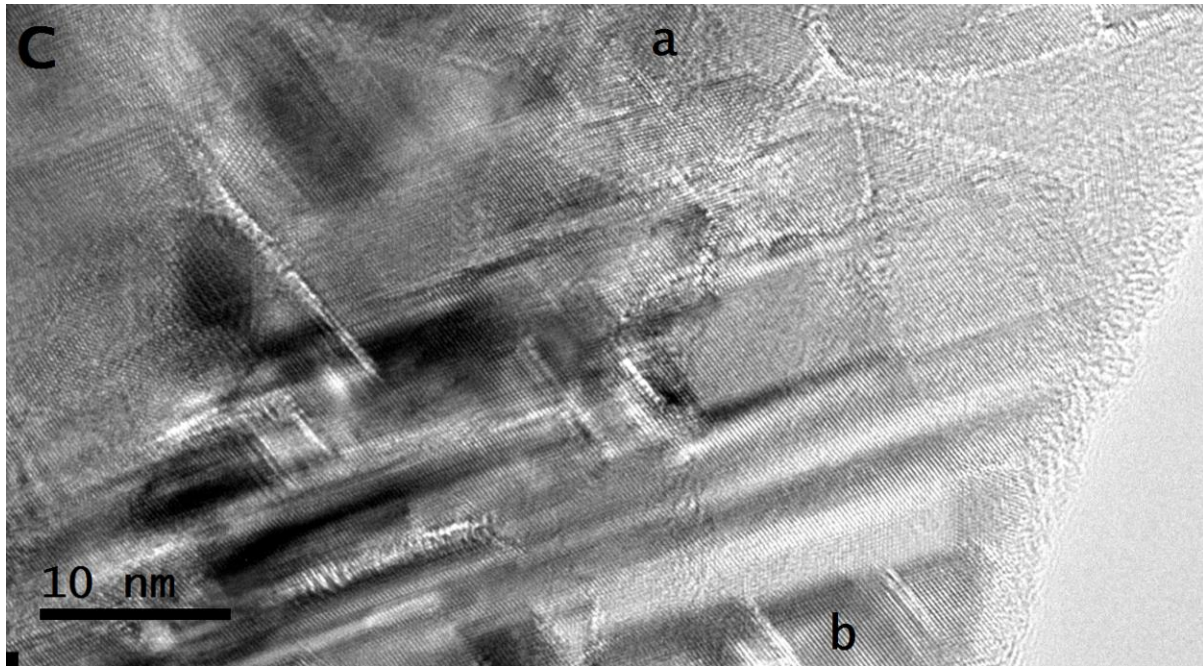


Figure 3: (a) Magnified view of the selected region of high-resolution transmission microscope image shows several overlaid tiny grains, (b) magnified view of the selected region of high-resolution transmission microscope image shows elongated atoms of graphite structure tiny grain and (c) standard high-resolution transmission microscope image shows large number of tiny grains developed in structure of smooth elements; ‘tiny grains carbon film’ synthesized at chamber pressure: 100 torr, mass flow rate: 200 sccm (6% H₂, 1 % CH₄ and 93 % argon), microwave power: 1400 (in watts) and deposition time: 60 minutes

Figure S7 shows high-resolution transmission microscope image taken from another region of the ‘tiny grains carbon film’, which highlights different features of the tiny grains. Gap between two tiny grains, which were developed into structure of smooth elements, labeled by (2) indicating canal-like channel and referred to ‘graphitic filament’ [39, 41]. High-resolution transmission microscope image taken from film synthesized at 200 torr is shown in Figure 4 (c), which indicates different phases of tiny grains. Two cropped regions of high-resolution image in magnified resolution are shown in Figures 4 (a) and 4 (b). In Figure 4 (a), tiny grains other than those developed into structure of smooth elements are shown. However, in Figure 4 (b), two tiny grains developed in structure of smooth elements are shown where a canal-like channel is formed between them. Different textures of tiny grains found in film are shown in Figure 4 (c), which also indicate different phases where less number of tiny grains developed structure into structure of smooth elements.

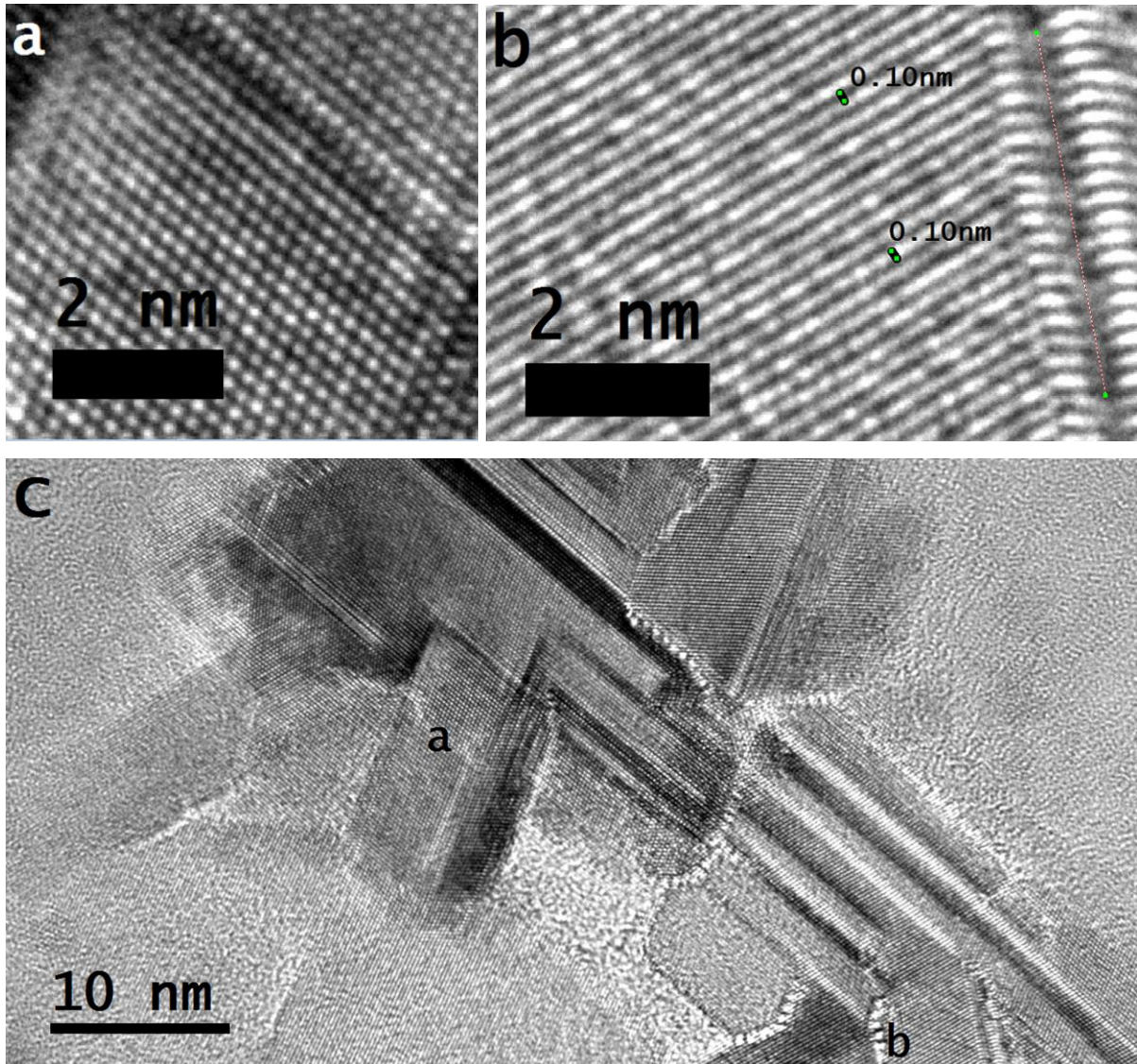


Figure 4: (a) Magnified view of the selected region of high-resolution transmission microscope image shows tiny grain of different phases where each phase is related to different state of carbon atoms, (b) magnified view of the selected region of high-resolution transmission microscope image shows tiny grain developed into structure of smooth elements and (c) standard high-resolution transmission microscope image shows different phase tiny grains comprised different state carbon atoms; 'tiny grains carbon film' synthesized at chamber pressure: 200 torr, mass flow rate: 200 sccm (6% H₂, 1 % CH₄ and 93 % argon), microwave power: 1400 (in watts) and deposition time: 60 minutes

From these high-resolution microscopic images, to identify state behavior of carbon atoms for different phases of tiny grains known in their exceptional hardness or other features is not in accordance to the application of microscope. However, it is visible to identify tiny grains evolved in graphitic state atoms as one-dimensional arrays converted to structure of smooth elements under the application of exerting surface format force, which are visible from topography view in all high-resolution transmission microscope images. Different state behavior of carbon atoms along

with binding of identical state atoms has been disclosed elsewhere [42]. In the case where atoms of tiny grains retain graphite structure and don't deal elongation due to certain aspects where remained hidden from the exertion of surface format forces, they encapsulated two-dimensional structure of graphitic state atoms too while amalgamating under attained dynamics, thus, evolve two-dimensional structure instead of one-dimensional structure. Further details of graphite structure when evolved under electron-dynamics by involving the non-conservative forces and when evolved only under attained dynamics of atoms is discussed elsewhere [42]. In 'tiny grains carbon films', propagation of photonic current is accelerated because of the naturally built-in channelized inter-state electron gap of their atoms. This is the cause of recognition of UNCD/NCD films in terms of enhanced field emission characteristics where inter-state electron gap works efficiently, thus, allowing propagation of accelerated current density of photons as discussed elsewhere [11]. This reveals that a tiny-sized particle or a quantum dot doesn't collectively oscillate on trapping or coupling light (photons), so, disregarding the largely studied phenomenon of surface plasmons or surface plasmon polaritons.

In Figures 5 (a) and (b), core loss PELS collected from the same region of 'tiny grains carbon films' at which high-resolution transmission microscope images were taken. An abrupt rise near 292 eV referred to σ^* -band and a large dip near 305 eV referred to tiny grains in diamond state [43, 44] and these bands are also found for the films synthesized at 100 torr and 200 torr as shown in Figures 5 (a) and (b). However, the large dip curve in both films which is more indicative in the case of film synthesized at 200 torr (Figure 5b) is due to energy band related to tiny grains elongated atoms to convert (and modify) into structure of smooth elements (~285 eV). The core loss PELS analysis of both films reveal the same peaks related to different energy bands and identical trend to the one observed in the case of Raman spectroscopy spectrum. But in the case of Raman spectroscopy analysis, the peaks' positions were at different wave numbers, whereas, in core loss PELS analysis the peaks' positions are at different energy bands; in the carbon film, different phases tiny grains evolved in lonsdaleite, diamond and graphene state atoms originating peaks at position of band energy ~295 (eV), ~308 (eV) and ~328 (eV), respectively. Those tiny grains of carbon film remained in fullerene state atoms reveal the decreasing level of energy in the form of dip curve at energy band ~ 304 (eV), which is notable in both films as shown in Figures 5 (a) and (b). In Figure 5 (a), more

pronounced hump-like peaks at ~328 eV is because of more number of tiny grains evolved in graphene state atoms.

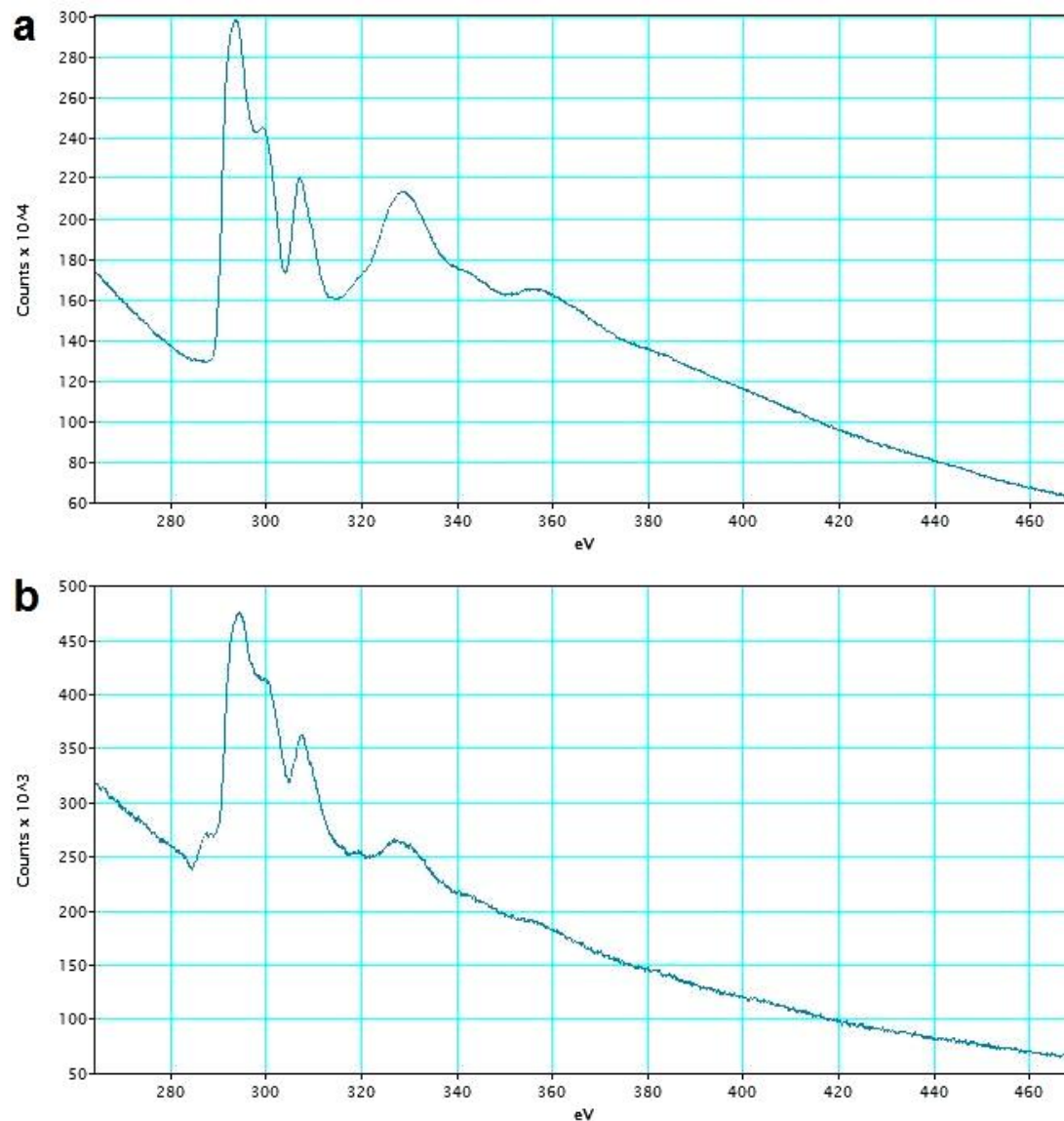


Figure 5: Core Loss PEELS analysis of 'tiny grains carbon films' synthesized at chamber pressure (a) 100 torr and (b) 200 torr; total mass flow rate: 200 sccm (6% H₂, 1 % CH₄ and 93 % argon), microwave power: 1400 (in watts) and deposition time: 60 minutes

In low loss EELS analysis, tiny grains of graphitic state atoms show a prominent peak at s_3 (27 eV), whereas, the a-C phase shows a peak at s_1 (22 eV) [44, 45]. However, in low loss PEELS shown in Figures 6 (a) and (b), a peak at 27 eV is not available in the analysis and energy band is at slightly titled position instead of to be at 22 eV, which is for both 'tiny grains carbon films', indicating the presence of different phases tiny grains in carbon films. Overall, the trend of peaks' behavior related to different band energy is in the same manner as analyzed in the case of

core loss PELS analysis of films. The built-in unit (eV) in the case of core loss PELS analysis and low loss PELS analysis are replaced with photon volts (pV).

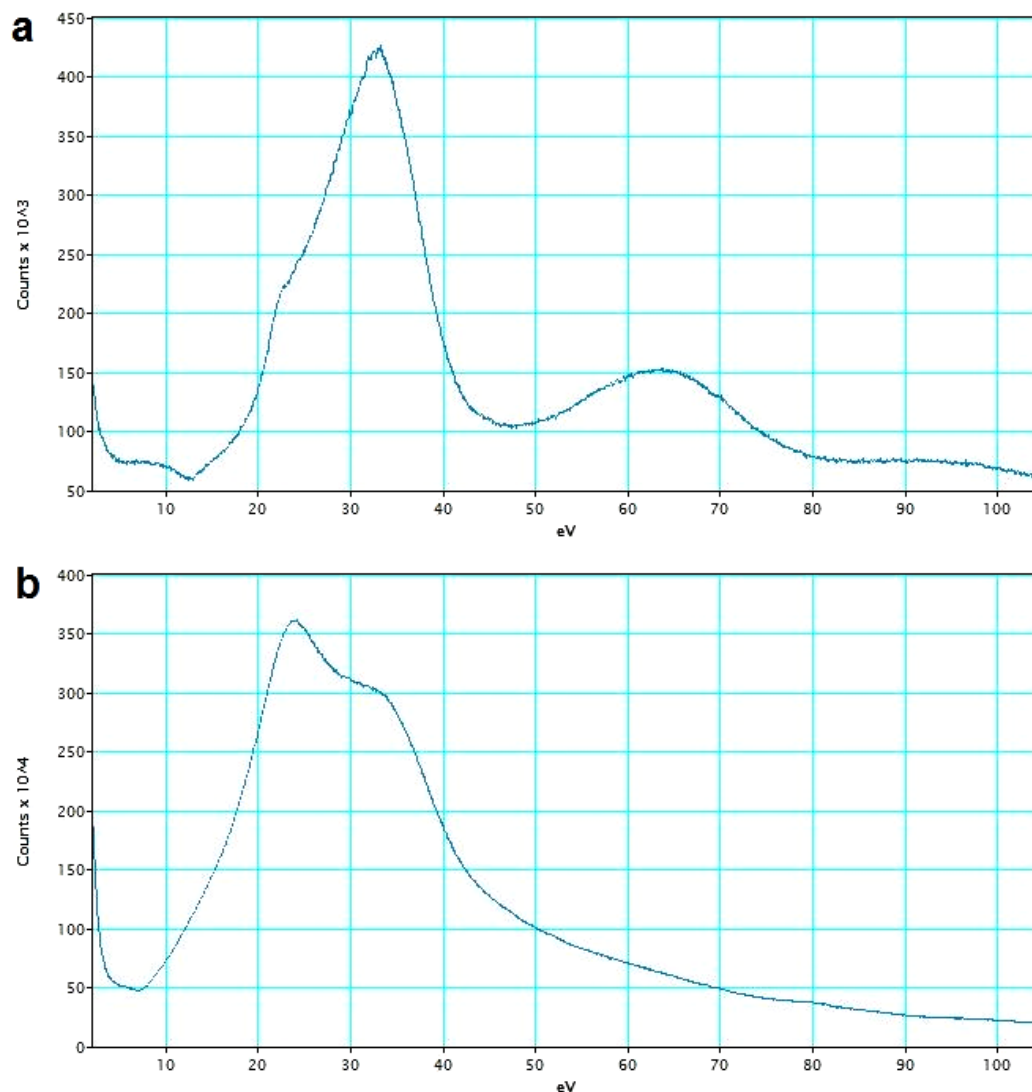


Figure 6: Low loss PELS analysis of ‘tiny grains carbon films’ synthesized at chamber pressure (a) 100 torr and (b) 200 torr; total mass flow rate: 200 sccm (6% H₂, 1 % CH₄ and 93 % argon), microwave power: 1400 (watts) and deposition time: 60 minutes

In Raman spectra of NCD/UNCD films, the peak at 1150 cm⁻¹ has been attributed to nanocrystalline diamond [45-47], however, the ‘v₁ peak’ (at 1150 cm⁻¹) can’t originate from a nanodiamond or related sp³-bonded phase but it is assigned to transpolyacetylene segments at grain boundaries and surfaces [48]. Nemanich *et al.* [46, 47] proposed that 1150 cm⁻¹ peak arises from nanocrystalline or amorphous diamond. In the Raman spectrum of NCD/UNCD film, the sharp peak at 1332.1 cm⁻¹ is the characteristic of diamond and broadening of the peak is related to the NCD grains [49]. In NCD/UNCD films, the peak at 1150 cm⁻¹ appears hypothetically due to CH bonds and is always linked to another peak at 1450 cm⁻¹, and the peaks at 1330

cm^{-1} and 1560 cm^{-1} are due to D-band and G-band [50], respectively. However, in the light of presented results of 'tiny grains carbon films', argon gas increased the rate of re-nucleation and the amount of tiny grains sizes $< 10 \text{ nm}$ enhanced significantly. Depending on how many tiny grains elongated atoms for structure of smooth elements, their quantity experienced Raman laser, the contribution recorded in the form of peak at wave number $\sim 1150 \text{ cm}^{-1}$. In microcrystalline diamond films, the size of grains is very large [1], thus, they don't retain graphite structure and diamond state atoms at a large extent evolving structure under the coordination of large amount of atomic hydrogen in HFCVD reactor as discussed elsewhere [13], accordingly, information put forth by Raman signals rather to record peak at 1150 cm^{-1} , the peak is recorded at 1332 cm^{-1} . Thus, the peak at wave number 1150 cm^{-1} is associated to those tiny grains which were developed in the graphite structure where their one-dimensional arrays of atoms dealt elongation of atoms resulting into develop the structure of smooth elements. Depending on the amount of tiny grains evolved in graphite structure followed by conversion in structure of smooth elements, the intensity of ' ν_1 peak' varied; different intensity of ' ν_1 peak' is related to the number of the tiny grains developed in structure of smooth elements experiencing the Raman laser. Those tiny grains evolved structure of fullerene state atoms become the origin of ' ν_2 peak' in the Raman spectrum. In this way, wherever the ' ν_1 peak' is resulted in the Raman spectrum of carbon films, the ' ν_2 peak' is resulted also. Incorporating H_2 in Ar-rich CH_4 mixture either eliminates the ' ν_1 peak' or it appears with less intensity. Without incorporation of H_2 in Ar-rich CH_4 mixture, ' ν_1 peak' is pronounced as shown in Figure S1. On varying concentration of feed gases, the scale of different phases of tiny grains is varied as well where counting different number of tiny grains developed in structure of smooth elements, thus, recorded different intensity of ' ν_1 peak' in the Raman spectrum. Again, different intensity of ' ν_1 peak' in same film is recorded on dealing Raman signals of different wavelength [51, 52] which is because of experiencing different level of signals of employed laser.

In Raman spectroscopy analysis, the peaks at different wave numbers are resulted because of the absorption of energy of interacting Raman laser in a different manner owing to different phases of tiny grains where atoms possessed different states of carbon as shown in Table 1; at wave number $\sim 1145 \text{ cm}^{-1}$, the ' ν_1 peak' is related to tiny grains of graphite phase evolved in graphitic state atoms where atoms of graphite structure elongated to develop structure of smooth elements and at wave

number $\sim 1310 \text{ cm}^{-1}$, the peak (due to D* band) is related to tiny grains evolved in lonsdaleite state atoms, and at wave number $\sim 1332 \text{ cm}^{-1}$, the peak (due to D band) is related to tiny grains evolved in diamond state atoms, and at wave number $\sim 480 \text{ cm}^{-1}$, the 'v₂ peak' is related to tiny grains evolved in fullerene state atom and at wave number $\sim 1580 \text{ cm}^{-1}$, the peak is related to tiny grains evolved in graphene state atoms.

Table 1: Raman and energy peaks of different phase tiny grains in carbon film

Elongated atoms graphite structure	Lonsdaleite structure	Diamond structure	Fullerene structure	Graphene structure
Raman spectroscopy (in cm⁻¹)				
v ₁ ~1145 (8734 nm)	D* ~1310 (7634 nm)	D ~1332 (7508 nm)	v ₂ ~1480 (6757 nm)	G ~1580 (6329 nm)
Core loss photon energy loss spectroscopy (in eV)				
Dip curve at ~285	Peak at ~295	Peak at ~308	Dip at ~304	Peak at ~328

In Table 1, wavelength of resulted Raman peak related to different phases of tiny grains available in the deposited film having different state of atoms for each phase is tabulated at different wave number (frequency). The lowest energy of those tiny grains was resulted which had elongated atoms of graphite structure, which is in the form of dip curve at ~ 285 (in eV) in their core loss PEELS analysis, thus, gives the longest recorded wavelength of 'v₁ peak' (~ 8734 nm) in the Raman spectrum analysis. On the other hand, where tiny grains evolved in graphene state atoms, the highest energy of the structure resulted at ~ 328 (in eV) in their core loss PEELS analysis, thus, gives the shortest wavelength (~ 6329 nm) in the Raman spectrum analysis. Those tiny grains work under the lowest energy and the longest wavelength (shortest wave number) of the structure resulted into the accelerated propagation of photonic current, which is termed as 'elongated atoms graphite structure' and availability of their greater content in the film guarantee the enhanced field emission characteristics.

In tiny grains of graphite structure, converted one-dimensional arrays of atoms to structure of smooth elements (elongated atoms graphite structure) further modified to shape smooth elements if the photons having adequate forcing energies travelling aside to their surface. Thus, such shaped tiny grains perfectly channelized the propagation of photonic current or other input signals under different wavelengths of

the laser. A travelling photon is related to forcing energy where energy of quantized amount is forced from one point to another point as discussed elsewhere [12].

As it is tabulated in the Table 1, tiny grains of 'elongated atoms graphite structure' give the highest value of wavelength indicating that they are the cause of enhanced field per unit length or area as discussed above. In the case of tiny grains having phase (state) of atoms in lonsdaleite, diamond and graphene, the decreased values of wavelength are resulted in respective manner. Now the question arises that recorded wavelength in the case of fullerene structure is also between diamond and graphene (in Table 1) but measured hardness is at very low level, however, the peak related to fullerene structure is at very low intensity in the Raman spectrum and we can observe associated energy in the form of dip curve in the spectrum of PELS. The scheme of electrons is different for different state carbon atoms [42], thus, each structure of established phase tiny grains delivers the different response against coordinated or interacted signals, which is distinctive for each carbon film. The cause of atoms of some elements to be in gas state and some to be in solid state is discussed elsewhere [53]. These findings also solicit to devise science of Raman spectroscopy and energy loss spectroscopy, accordingly.

4.0 Conclusions

'Tiny grains carbon films' comprise different phases of tiny grains under different converted state of carbon atoms. A 'tiny grains carbon film' synthesized under suitable conditions in microwave-based vapor deposition system evolves 'elongated atoms graphite structure', also. In tiny grains where graphitic state atoms bind under the execution of electron-dynamics elongated atoms of one-dimensional arrays to structure of smooth elements while exerting surface format force from their centers along opposite poles. Such tiny grains are the cause of 'v₁ peak' in the Raman spectrum where the lowest wave number is resulted due to enhanced field emission performance under the accelerated rate of current density. In the case of tiny grains where carbon atoms converted to fullerene state, they are related to 'v₂ peak' in the Raman spectrum. Results of field emission measurements of films synthesized at different pressure are in-match to energy loss spectroscopy and Raman spectroscopy analyses. In Raman spectroscopy and energy loss spectroscopy analyses, the peaks related to different wave numbers and energy bands are

because of propagation of input energy signals through inter-state electron gap of different state atoms tiny grains evolved in different phases in the carbon film.

Traveling photons of adequate wavelength aside to the surface of tiny grains having 'elongated atoms graphite structure' further shape to structure of smooth elements as per forcing energies, thus, enabling enhanced and accelerated propagation of field under the capacity of different input sources where such tiny grains also negating phenomenon of surface plasmon polaritons.

Our experimental results well prove and justify the position of peaks related to different state carbon atoms tiny grains evolved into different phases in their films synthesized under different conditions in microwave-based vapor deposition system and in good agreement to field emission characteristics. In line with this, present studies set a new horizon in synthesizing, analyzing and evaluating materials at nanoscale, and soliciting reinvestigation of materials' syntheses and their performances both for existing and future applications.

Acknowledgements:

Mubarak Ali thanks National Science Council (now MOST) Taiwan (R.O.C.) for awarding postdoctorship: NSC-102-2811-M-032-008 (2013-2014). Authors wish to thank Mr. Tsung-Min Chen for assisting films' synthesis and Mr. Chien-Jui Yeh in TEM operation.

References:

- [1] M. Ali, M. Ürgen, Switching dynamics of morphology-structure in chemically deposited carbon films -A new insight, *Carbon* 122 (2017) 653-663.
- [2] S. Link, M. A. El-Sayed, Shape and size dependence of radiative, nonradiative and photothermal properties of gold nanocrystals, *Int. Rev. Phys. Chem.* 19 (2000) 409- 453.
- [3] S. C. Glotzer, M. J. Solomon, Anisotropy of building blocks and their assembly into complex structures, *Nature Mater.* 6 (2007) 557-562.
- [4] M. Ali, I –N. Lin, The effect of the Electronic Structure, Phase Transition and Localized Dynamics of Atoms in the formation of Tiny Particles of Gold, <http://arXiv.org/abs/1604.07144>.
- [5] M. Ali, I –N. Lin, Development of gold particles at varying precursor concentration, <http://arxiv.org/abs/1604.07508>.

- [6] M. Ali, I –N. Lin, Tapping opportunity of tiny shaped particles and role of precursor in developing shaped particles, <http://arxiv.org/abs/1605.02296>.
- [7] M. Ali, I –N. Lin, Controlling morphology-structure of particles at different pulse rate, polarity and effect of photons on structure, <http://arxiv.org/abs/1605.04408>.
- [8] M. Ali, I –N. Lin, Formation of tiny particles and their extended shapes – Origin of physics and chemistry of materials, <http://arxiv.org/abs/1605.09123>.
- [9] M. Ali, Structure evolution in atoms of solid state dealing electron transitions. <http://arxiv.org/abs/1611.01255>.
- [10] M. Ali, The study of tiny shaped particle dealing localized gravity at solution surface. <http://arxiv.org/abs/1609.08047>.
- [11] M. Ali, Atoms of electronic transition deform or elongate but do not ionize while inert gas atoms split. <http://arxiv.org/abs/1611.05392>.
- [12] M. Ali, Revealing the Phenomena of Heat and Photon Energy on Dealing Matter at Atomic level. <https://www.preprints.org/manuscript/201701.0028/v10>.
- [13] M. Ali, M. Ürgen, Deposition Chamber Pressure on the Morphology of Carbon Films (2018). <https://arxiv.org/abs/1802.00730>
- [14] M. Ali, Nanoparticles-Photons: Effective or Defective Nanomedicine, J. Nanomed. Res. 5 (2017): 00139.
- [15] W. Zhu, G. P. Kochanski, S. Jin, Low-Field Electron Emission from Undoped Nanostructured Diamond, Science 282 (1998) 1471-1473.
- [16] J. Birrell, J. A. Carlisle, O. Auciello, D. M. Gruen, J. M. Gibson, Morphology and electronic structure in nitrogen-doped ultrananocrystalline diamond, Appl. Phys. Lett. 81 (2002) 2235-2237.
- [17] J. E. Dahl, S. G. Liu, R. M. K. Carlson, Isolation and Structure of Higher Diamondoids, Nanometer-Sized Diamond Molecules, Science 299 (2003) 96-99.
- [18] J. Y. Raty, G. Galli, Ultradispersity of diamond at the nanoscale, Nature Mater. 2 (2003) 792-795.
- [19] S. C. Tjong, H. Chen, Nanocrystalline materials and coatings, Mater. Sci. Engineer. R 45 (2004) 1-88.
- [20] A. V. Sumant *et al.*, Towards the Ultimate Tribological Interface: Surface Chemistry and Nanotribology of Ultrananocrystalline Diamond, Adv. Mater. 17 (2005) 1039-1045.

- [21] A. R. Krauss, O. Auciello, M. Q. Ding, D. M. Gruen, Y. Huang, V. V. Zhirnov, E. I. Givargizov, A. Breskin, R. Chechen, E. Shefer, V. Konov, S. Pimenov, A. Karabutov, A. Rakhimov, N. Suetin, Electron field emission for ultrananocrystalline diamond films, *J. Appl. Phys.* 89 (2001) 2958-2967.
- [22] X. Xiao, J. Birrell, J. E. Gerbi, O. Auciello, J. A. Carlisle, Low temperature growth of ultrananocrystalline diamond, *J. Appl. Phys.* 96 (2004) 2232-2239.
- [23] O. A. Williams, M. Nesladek, M. Daenen, S. Michaelcon, A. Hoffman, E. Osawa, K. Haenen, R. B. Jackman, Growth, electronic properties and applications of nanodiamond, *Diam. Relat. Mater.* 17 (2008) 1080-1088.
- [24] A. R. Konicek, D. S. Grierson, P. U. P. A. Gilbert, W. G. Sawyer, A. V. Sumant, R. W. Carpick, Origin of Ultralow Friction and Wear in Ultrananocrystalline Diamond, *Phys. Rev. Lett.* 100 (2008) 235502-04.
- [25] J. E. Butler, A. V. Sumant, The CVD of Nanodiamond Materials, *Chem. Vap. Deposition* 14 (2008) 145-160.
- [26] J. P. Thomas, H. C. Chen, N. H. Tai, I -N. Lin, Freestanding Ultrananocrystalline Diamond Films with Homo Junction Insulating Layer on Conducting Layer and Their High Electron Field Emission Properties, *ACS Appl Mater Interfaces* 3 (2011) 4007-4013.
- [27] W. Kulisch, C. Petkov, E. Petkov, C. Popov, P. N. Gibson, M. Veres, R. Merz, B. Merz, J. P. Reithmaier, Low temperature growth of nanocrystalline and ultrananocrystalline diamond films: A comparison, *Phys. Status Solidi A* 209 (2012) 1664-1674.
- [28] K. J. Sankaran *et al.*, Improvement in plasma illumination properties of ultrananocrystalline diamond films by grain boundary engineering, *J. Appl. Phys.* 114 (2013) 054304-11.
- [29] K. J. Sankaran *et al.*, Improvement in Tribological Properties by Modification of Grain Boundary and Microstructure of Ultrananocrystalline Diamond Films, *ACS Appl. Mater. Interfaces* 5 (2013) 3614-3624.
- [30] A. Saravanan *et al.*, Fast growth of ultrananocrystalline diamond films by bias-enhanced nucleation and growth process in CH₄/Ar plasma, *Appl. Phys. Lett.* 104 (2014) 181603-5.
- [31] C. S. Wang, H. C. Chen, H. F. Cheng, I -N. Lin, Origin of platelike granular structure for the ultrananocrystalline diamond films synthesized in H₂ - containing Ar / CH₄ plasma, *J. Appl. Phys.* 107 (2014) 034304-7.

- [32] H. Zeng *et al.*, Boron-doped ultrananocrystalline diamond synthesized with an H-rich/Ar-lean gas system, *Carbon* 84 (2015) 103-117.
- [33] K. J. Sankaran, K. Panda, B. Sundaravel, H. –C. Chen, I –N. Lin, C. –Y. Lee, N. –H. Tai, Engineering the Interface Characteristics of Ultrananocrystalline Diamond Films Grown on Au-Coated Si Substrates, *ACS Appl. Mater. Interfaces* 4 (2012) 4169-4176.
- [34] J. P. Thomas *et al.*, Preferentially Grown Ultrananocrystalline c-Diamond and n-Diamond Grains on Silicon Nanoneedles from Energetic Species with Enhanced Field-Emission Properties, *ACS Appl. Mater. Interfaces* 4 (2012) 5103-5108.
- [35] K. J. Sankaran, H. –C. Chen, K. Panda, B. Sundaravel, C. –Young Lee, N. –H. Tai, I –N. Lin, Enhanced Electron Field Emission Properties of Conducting Ultrananocrystalline Diamond Films after Cu and Au Ion Implantation, *ACS Appl. Mater. Interfaces* 6 (2014) 4911-4919.
- [36] K. J. Sankaran, K. Panda, B. Sundaravel, N. H. Tai, I –N. Lin, Enhancing electrical conductivity and electron field emission properties of ultrananocrystalline diamond films by copper ion implantation and annealing, *J. Appl. Phys.* 115 (2014) 063701-7.
- [37] K. J. Sankaran *et al.*, Electron Field Emission Enhancement of Vertically Aligned Ultrananocrystalline Diamond-Coated ZnO Core–Shell Heterostructured Nanorods, *Small* 10 (2014) 179-185.
- [38] Y. Tzeng, S. Yeh, W. C. Fang, Y. Chu, Nitrogen-incorporated ultrananocrystalline diamond and multi-layer-graphene-like hybrid carbon films, *Sci. Rep.* 4 (2014) 4531.
- [39] S. C. Lin *et al.*, The microstructural evolution of ultrananocrystalline diamond films due to P ion implantation and annealing process-dosage effect, *Diam. Relat. Mater.* 54 (2015) 47-54.
- [40] K. Panda, E. Inami, Y. Sugimoto, K. J. Sankaran, I –Nan Lin. Straight imaging and mechanism behind grain boundary electron emission in Pt-doped ultrananocrystalline diamond films. *Carbon* 111 (2017) 8-17.
- [41] A. Saravanan, B. R. Huang, K. J. Sankaran, G. Keiser, J. Kurian, N. H. Tai, I. N. Lin, Structural modification of nanocrystalline diamond films via positive/negative bias enhanced nucleation and growth processes for improving their electron field emission properties, *J. Appl. Phys.* 117 (2015) 215307-11.

- [42] M. Ali, Atomic Structure and Binding of Carbon Atoms, (2018).
<https://www.preprints.org/manuscript/201801.0036/v2>
- [43] D. M. Gruen, S. Liu, A. R. Krauss, X. Pan, Buckyball microwave plasmas: Fragmentation and diamond-film growth, *J. Appl. Phys.* 75 (1994) 1758-1763.
- [44] P. Kovarik, E. B. D. Bourdon, R. H. Prince, Electron-energy-loss characterization of laser-deposited *a*-C, *a*-C:H, and diamond films, *Phys. Rev. B* 48 (1993) 12123-12129.
- [45] W. A. Yarbrough, R. Messier, Current issues and problems in the chemical vapor deposition of diamond, *Science* 247 (1990) 688-696.
- [46] R. J. Nemanich, J. T. Glass, G. Lucovsky, R. E. Shroder, Raman scattering characterization of carbon bonding in diamond and diamondlike thin films, *J. Vac. Sci. Technol. A* 6 (1988) 1783-1787.
- [47] R. E. Shroder, R. J. Nemanich, J. T. Glass, Analysis of the composite structures in diamond thin films by Raman spectroscopy, *Phys. Rev. B* 41 (1990) 3738-3745.
- [48] A. C. Ferrari, J. Robertson, Origin of the 1150cm^{-1} Raman mode in nanocrystalline diamond, *Phys. Rev. B* 63 (2001) 121405-5.
- [49] I. Jiménez, M. M. García, J. M. Albella, L. J. Terminello, Orientation of graphitic planes during the bias-enhanced nucleation of diamond on silicon: An x-ray absorption near-edge study, *Appl. Phys. Lett.* 73 (1998) 2911-2913.
- [50] J. Birrell, J. E. Gerbi, O. Auciello, J. M. Gibson, J. Johnson, J. A. Carlisle, Interpretation of the Raman spectra of ultrananocrystalline diamond, *Diam. Relat. Mater.* 14 (2005) 86-92.
- [51] R. Haubner, M. Rudigier, Raman characterisation of diamond coatings using different laser wavelengths, *Physics Procedia* 46 (2013) 71-78.
- [52] S. C. Ray, I –N. Lin, Ferroelectric behaviours of ultra-nano-crystalline diamond thin films, *Surf. Coat. Technol.* 271 (2015) 247-250.
- [53] M. Ali. Why Atoms of Some Elements are in Gas State and Some in Solid State, but Carbon Works on Either Side, (2018).
<https://www.preprints.org/manuscript/201803.0092/v1>

Authors' biography:



Mubarak Ali graduated from University of the Punjab with B.Sc. (Phys& Maths) in 1996 and M.Sc. Materials Science with distinction at Bahauddin Zakariya University, Multan, Pakistan (1998); thesis work completed at Quaid-i-Azam University Islamabad. He gained Ph.D. in Mechanical Engineering from Universiti Teknologi Malaysia under the award of Malaysian Technical Cooperation Programme (MTCP;2004-07) and postdoc in advanced surface technologies at Istanbul Technical University under the foreign fellowship of The Scientific and Technological Research Council of Turkey (TÜBİTAK; 2010). He completed another postdoc in the field of nanotechnology at Tamkang University Taipei (2013-2014) sponsored by National Science Council now M/o Science and Technology, Taiwan (R.O.C.). Presently, he is working as Assistant Professor on tenure track at COMSATS Institute of Information Technology, Islamabad campus, Pakistan (since May 2008) and prior to that worked as assistant director/deputy director at M/o Science & Technology (Pakistan Council of Renewable Energy Technologies, Islamabad; 2000-2008). He was invited by Institute for Materials Research (IMR), Tohoku University, Japan to deliver scientific talk on growth of synthetic diamond without seeding treatment and synthesis of tantalum carbide. He gave several scientific talks in various countries. His core area of research includes materials science, physics & nanotechnology. He was also offered the merit scholarship (for PhD study) by the Government of Pakistan but he couldn't avail. He is author of several articles published in various periodicals (<https://scholar.google.com.pk/citations?hl=en&user=UYjvhDwAAAAJ>).



I-Nan Lin is a senior professor at Tamkang University, Taiwan. He received the Bachelor degree in physics from National Taiwan Normal University, Taiwan, M.S. from National Tsing-Hua University, Taiwan, and the Ph.D. degree in Materials Science from U. C. Berkeley in 1979, U.S.A. He worked as senior researcher in Materials Science Centre in Tsing-Hua University for several years and now is faculty in Department of Physics, Tamkang University. Professor Lin has more than 200 referred journal publications and holds top position in his university in terms of research productivity. Professor I-Nan Lin supervised several PhD and Postdoc candidates around the world. He is involved in research on the development of high conductivity diamond films and on the transmission microscopy of materials.

Supplementary Materials:

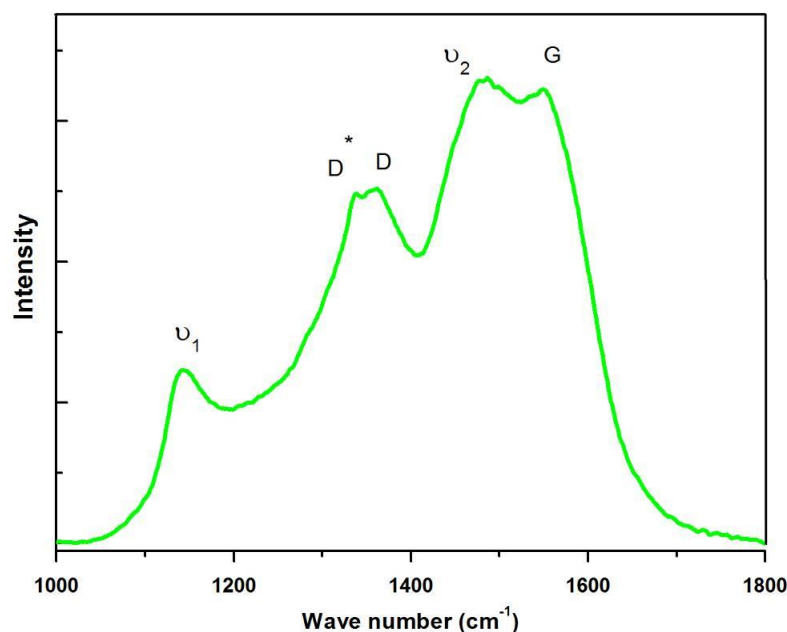


Figure S1: Raman spectrum of 'tiny grains carbon film' synthesized at chamber pressure 150 torr; total mass flow rate: 200 sccm (0% H₂, 2 % CH₄ and 98 % argon, Ar: CH₄: H₂ = 196:4:0), microwave power: 1100 (in watts) and deposition time: 60 minutes (ν_1 : ~1145 cm⁻¹, D*: ~1310 cm⁻¹, D: 1332 cm⁻¹, ν_2 : ~1480 cm⁻¹, G: ~1580 cm⁻¹)

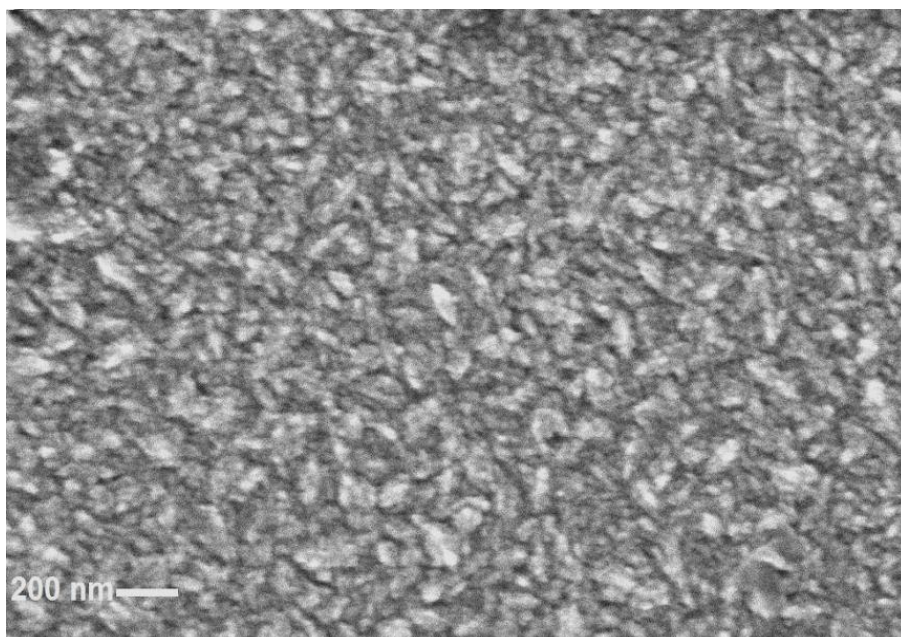
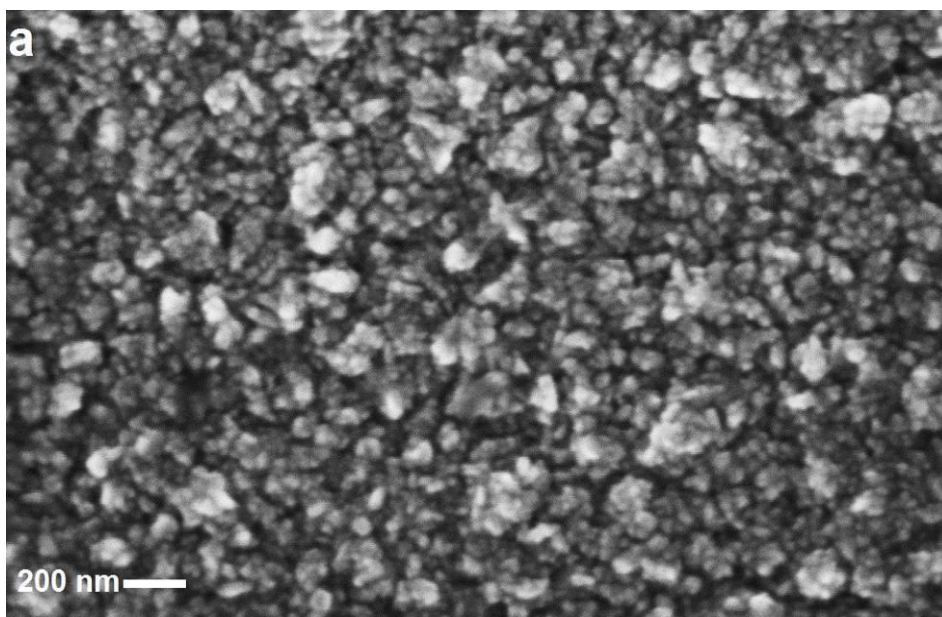


Figure S2: Surface morphology of 'tiny grains carbon film' synthesized at chamber pressure 150 torr; total mass flow rate: 200 sccm (0% H₂, 2 % CH₄ and 98 % argon, Ar: CH₄: H₂ = 196:4:0), microwave power: 1100 (in watts) and deposition time: 60 minutes



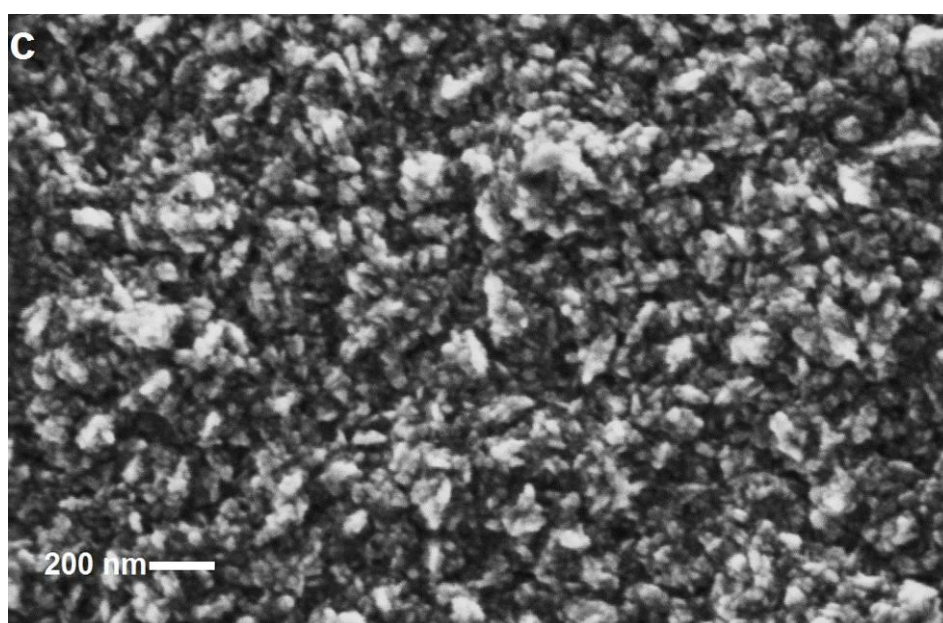
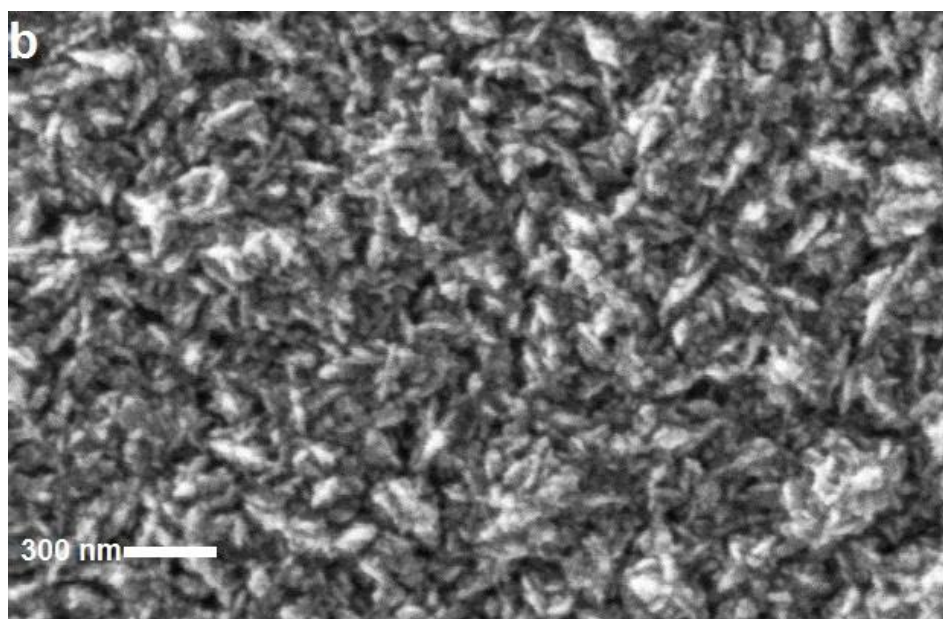
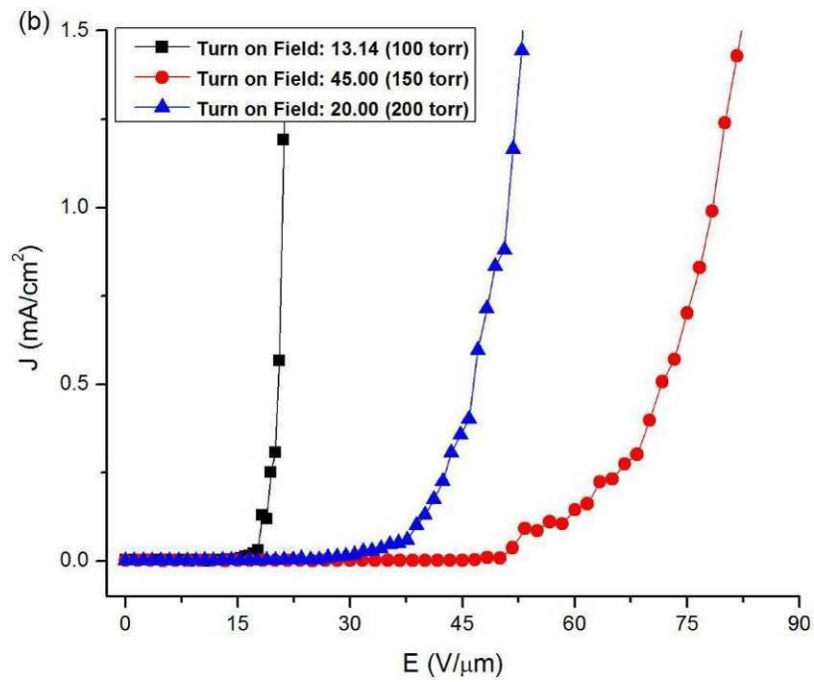
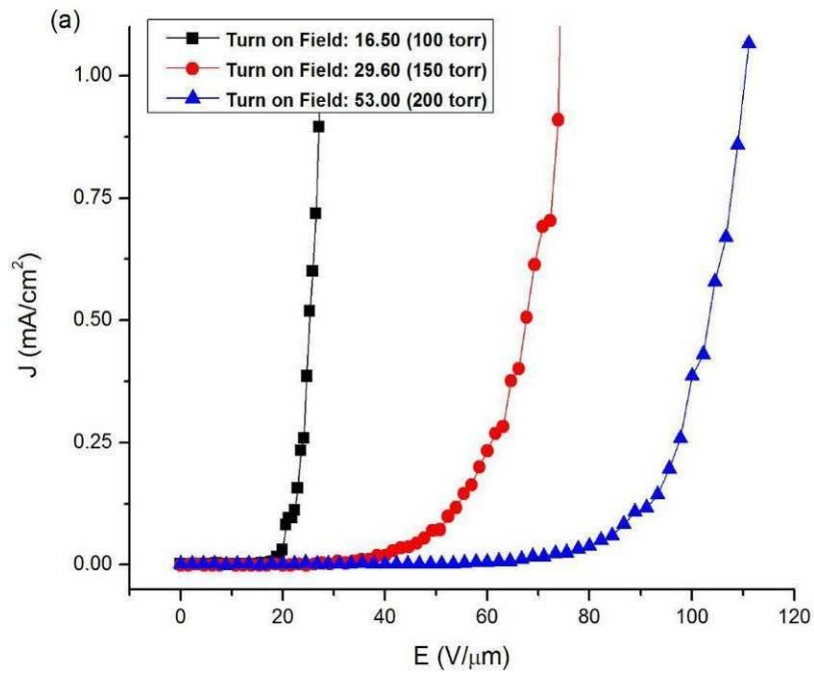


Figure S3: Surface morphology of 'tiny grains carbon films' synthesized at chamber pressure (a) 100 torr, (b) 150 torr, and (c) 200 torr; total mass flow rate: 200 sccm (6% H₂, 1 % CH₄ and 93 % argon, Ar: CH₄: H₂ = 186:2:12), microwave power: 1400 (in watts) and deposition time: 60 minutes



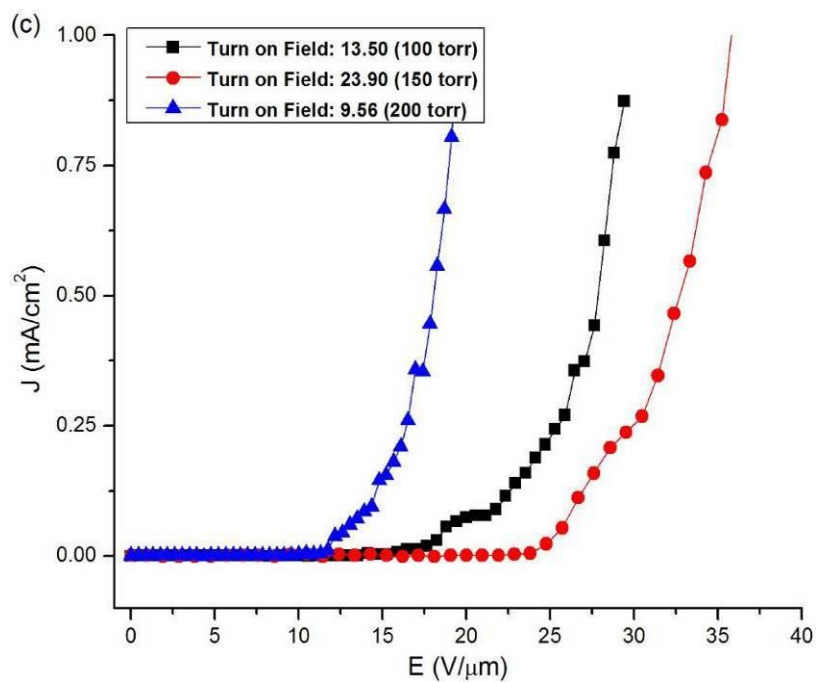
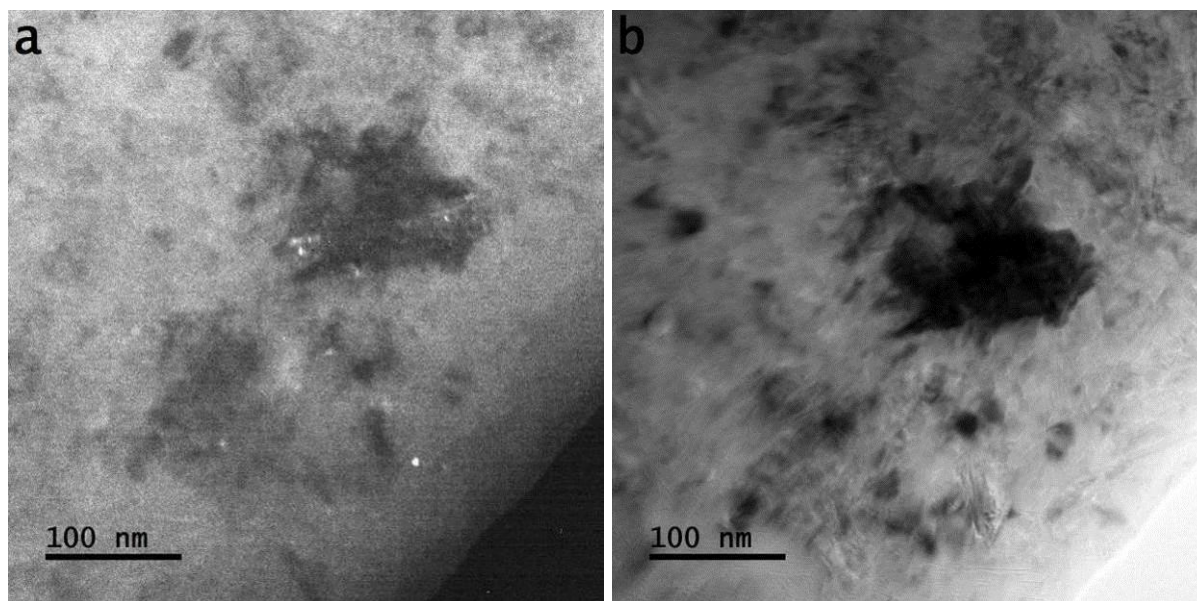


Figure S4: Field emission current density as a function of applied field of 'tiny grains carbon films' synthesized (a) without H₂, (b) with 3 % H₂ and (c) with 6 % H₂; 1 % CH₄, total mass flow rate: 200 sccm, microwave power: 1200 (in watts) and deposition time: 60 minutes



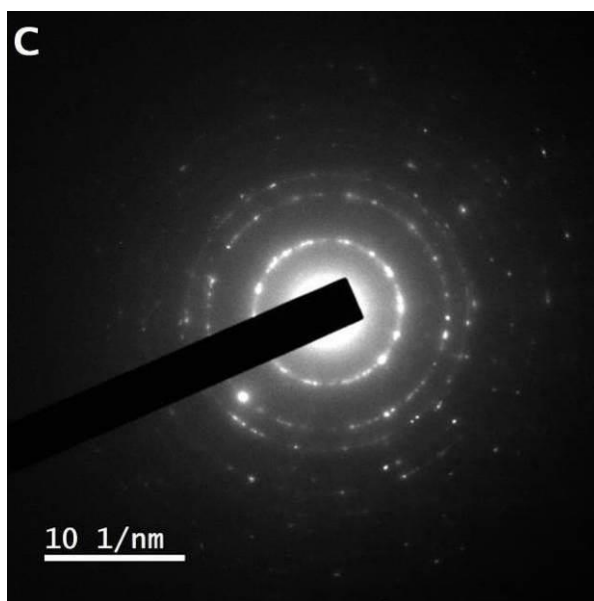
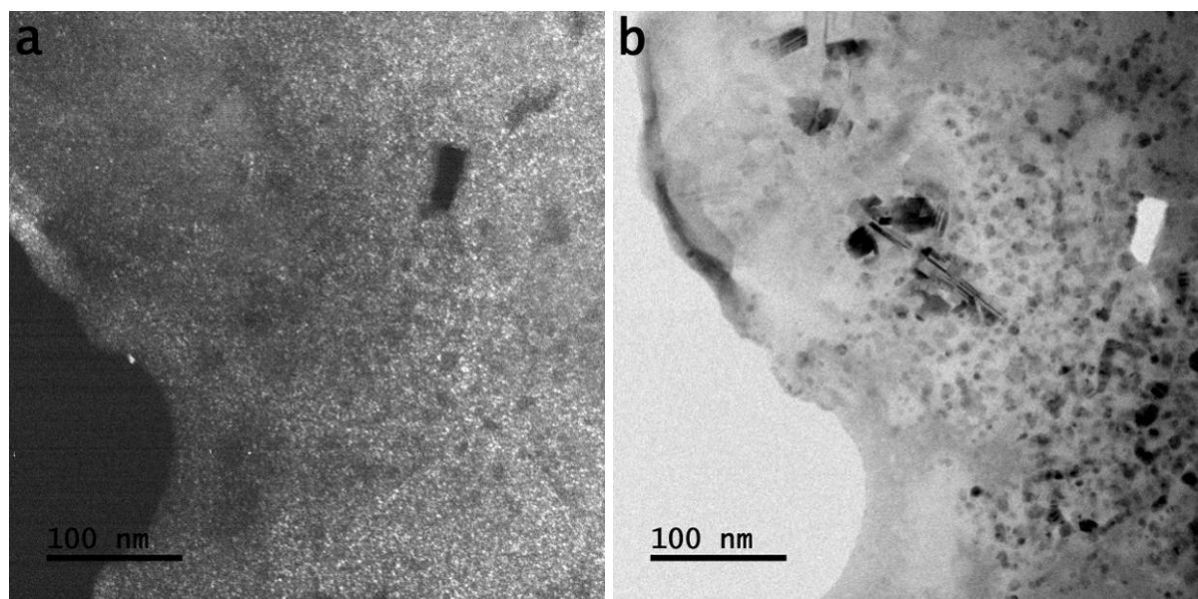


Figure S5: (a) Dark field transmission microscope image (b) bright field transmission microscope image and (c) SAPR pattern of 'tiny grains carbon film' synthesized at chamber pressure: 100 torr, total mass flow rate: 200 sccm (6% H₂, 1 % CH₄ and 93 % argon), microwave power: 1400 watts (in watts) and deposition time: 60 minutes



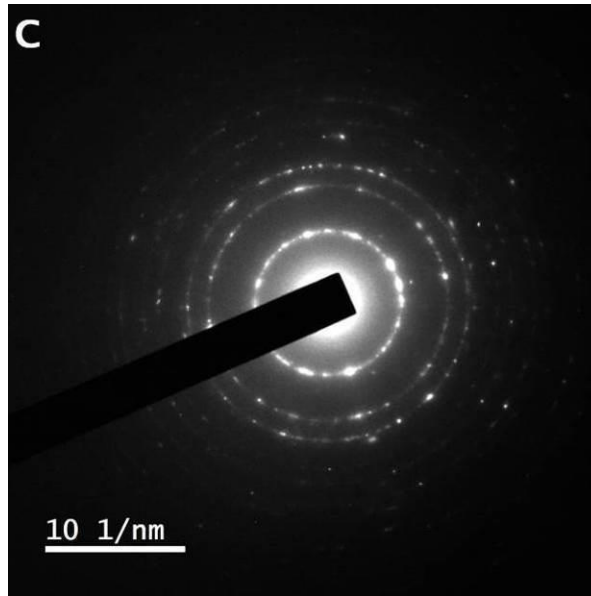


Figure S6: (a) Dark field transmission microscope image (b) bright field transmission microscope image and (c) SAPR pattern of 'tiny grains carbon film' synthesized at chamber pressure: 200 torr, total mass flow rate: 200 sccm (6% H₂, 1 % CH₄ and 93 % argon), microwave power: 1400 (in watts) and deposition time: 60 minutes

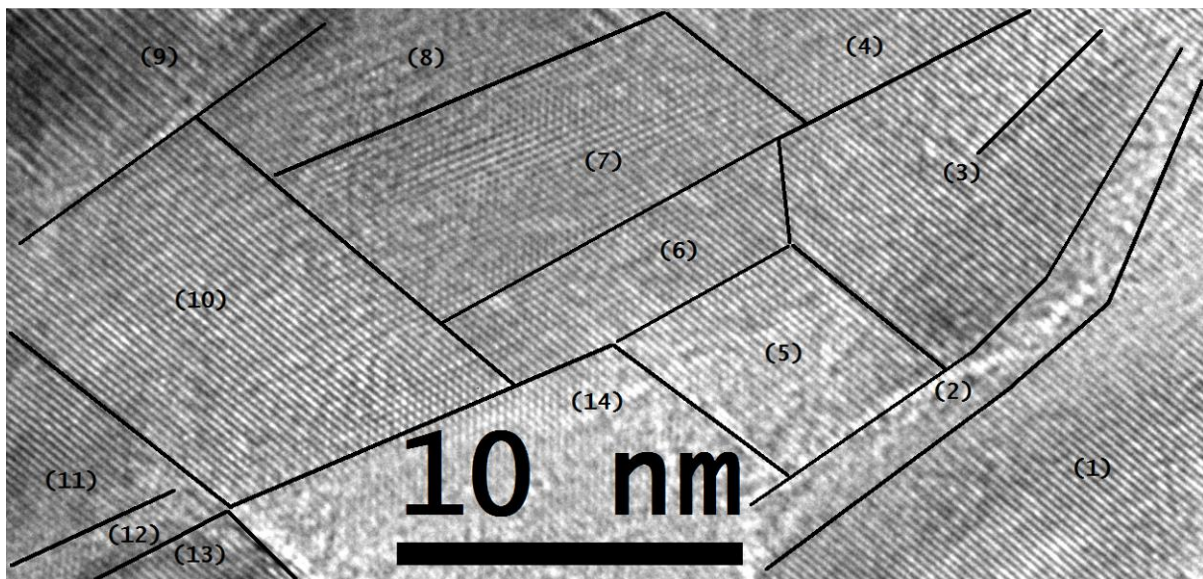


Figure S7: High-resolution transmission microscope image of carbon film synthesized at chamber pressure 100 torr shows different phases of tiny grains evolved in different states of carbon atoms; total mass flow rate: 200 sccm (6% H₂, 1 % CH₄ and 93 % argon), microwave power: 1400 (in watts) and deposition time: 60 minutes